

Performance of a Graphite Foam Thermosyphon for Cooling Integrated Circuits

James Klett, Mike Trammell
Metals and Ceramics Division, Oak Ridge National Laboratory
Oak Ridge, TN, 37831
klettjw@ornl.gov

Background

Current CMOS (complementary metal-oxide semiconductors) type microelectronics, such as computer microprocessors, experience power densities over 50 W/cm^2 and are cooled effectively with aluminum and copper heat sinks. However, as technology improves, high performance microprocessors will likely experience power densities over 200 W/cm^2 .

The “flip-chip” design currently used in today’s microprocessors has inherent problems. Here, the silicon die is inverted with the back of the printed chip oriented towards the top of the package. In this case, the integrated heat spreader (IHS) can be joined directly to the silicon chip and cooled with a finned air cooled heat sink. Unfortunately, as the power increases above 100W, this can result in temperatures in excess of 85°C on the printed active layer in the chip, reducing reliability and shortening life.

Current research has focus on the thermosyphon design [1] where the heat sink bonded to the chip is immersed in an evaporative cooling fluid (e.g. fluorocarbon, FC-87, FC-72). The latent heat of vaporization of the cooling fluid removes significantly more heat than the sensible heat change of the fluid while transferring the heat efficiently to fins of a condenser. The performance of the evaporative coolers is currently limited by the surface area and thermal conductivity of the spreader mounted to the back of the chip.

Recently, high thermal conductivity graphite foams have been demonstrated to be efficient evaporators for these type of thermosyphons. The very high ligament conductivity combined with very high surface areas (compared to standard IHS’s) yields an evaporator which is capable of dissipating even greater heat fluxes than state of the art devices.

Experimental

A thermosyphon chamber was built at ORNL, Figure 1, to measure the performance of the graphite foam as an evaporator. The system developed to investigate microelectronic CMOS chip cooling, shown in Figure 3, consists of the following components: (a) a silicon die with a resistor as the printed active layer, (b) a block of graphite foam measuring $2.5 \times 2.5 \times 1 \text{ cm}$ mounted to the chip by soldering (c) a pin grid array (PGA) mounted and wire bonded to the chip by Laboratory for Physical Sciences at the University of Maryland, (d) an aluminum holder attached to the chip assembly using RTV sealant, (e) a zero insertion force (ZIF) socket attached to a circuit board, (f) a circuit board and wiring, (g) a glass walled chamber with aluminum flanges, (h) a fluid bubbler for de-airing the Fluorinert, (i) a water cooled condenser, (j) a 1000W power supply, (k) type-K thermocouples, (l) 4 multimeters for measuring resistance of

temperature sensitive resistors printed on the active layer, and (m) Swagelok valve and fittings.

To characterize the effects of foam geometries on the performance of the thermosyphon, two silicon chips (dies 1 cm x 1 cm) with similar density foams bonded to them were individually characterized with Fluorinert FC-87 and repeated for validation. The power, q'' , was increased in 10W increments until 150 W or chip temperature (active layer) of 90°C was reached. For each power level, the system was allowed to run for 15 minutes to equilibrate and the four resistor temperatures and vapor saturation temperature, T_{sat} were recorded. From the temperature from the resistors on the active layer and the saturation temperature of the vapor, the degree of superheat, ΔT_{SH} , was calculated and plotted against the heat flux (Figure 2).

To evaluate the effect of foam geometry on the performance of the system, the evaporators for the two chips (chips 3 and 4) were machined into a slotted pattern (6.25 mm x 6.25 mm) and the performance was measured. Figure 2 illustrates the machined slotted pattern in Chip 4 (before and after machining).

Figure 3 shows that for both chips, the slotted geometry pattern produces lower superheats at similar heat fluxes, indicating significant performance improvements over the solid evaporator. In fact, chip 4 was able to dissipate 150 W/cm² at a modest superheat of only 11°C. Note that the incipience from nucleate boiling to pool boiling in Chip 4 was still around 1-2°C, but the heat flux at this point was increased from about 5 to 40 W/cm². The slotted pattern may increase the effectiveness of the convection cooling such that higher heat fluxes can be attained before pool boiling occurs. This improvement is likely related to the total surface area of the slotted fins. It is also important to note that critical heat flux [ref], CHF, was not experienced for the solid or slotted foam evaporators.

The most significant result of these tests may be that the actual temperature of the active layer, Figure 4, was less than 71°C for chip 4 and approximately 90°C for chip 3. Therefore, this demonstrated that a printed active layer temperature less than the desired 85°C can be attainable at powers as high as 150 W/cm² using the graphite foam. The performance of the graphite foam evaporators are compared to state-of-the-art thermosyphons in Table 1. As can be seen, the boiling thermal resistance, $\Delta T_{\text{SH}}/q''$, of the graphite foams was better than all other cooling techniques, including spray cooling (the typical benchmark in advanced cooling).

Conclusions

Graphite foam serves as an excellent evaporator compared to traditional evaporators in thermosyphons. The graphite foam was demonstrated to dissipate up to 150 W/cm² at superheats of only 11°C. In addition, these graphite foam thermosyphons have demonstrated that the temperature of the active layer of the CMOS can be below 85C during these very high heat fluxes. These systems were even better than the state-of-the-art-cooling systems.

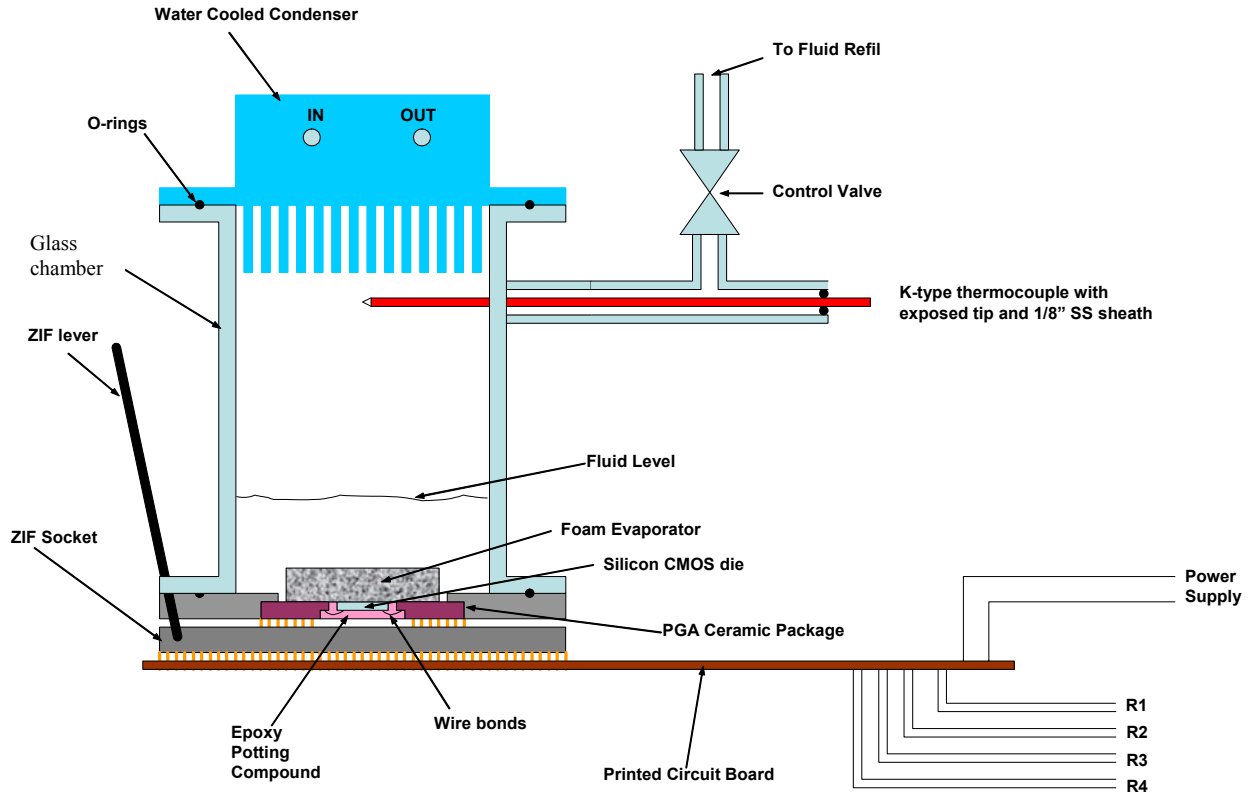


Figure 1. Schematic of setup

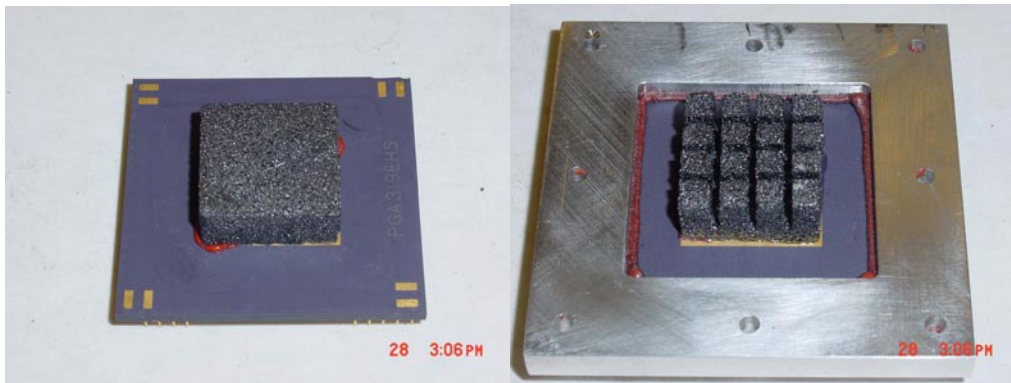


Figure 2. Images of the graphite foam evaporator bonded to chip 4 with and without machined slots.

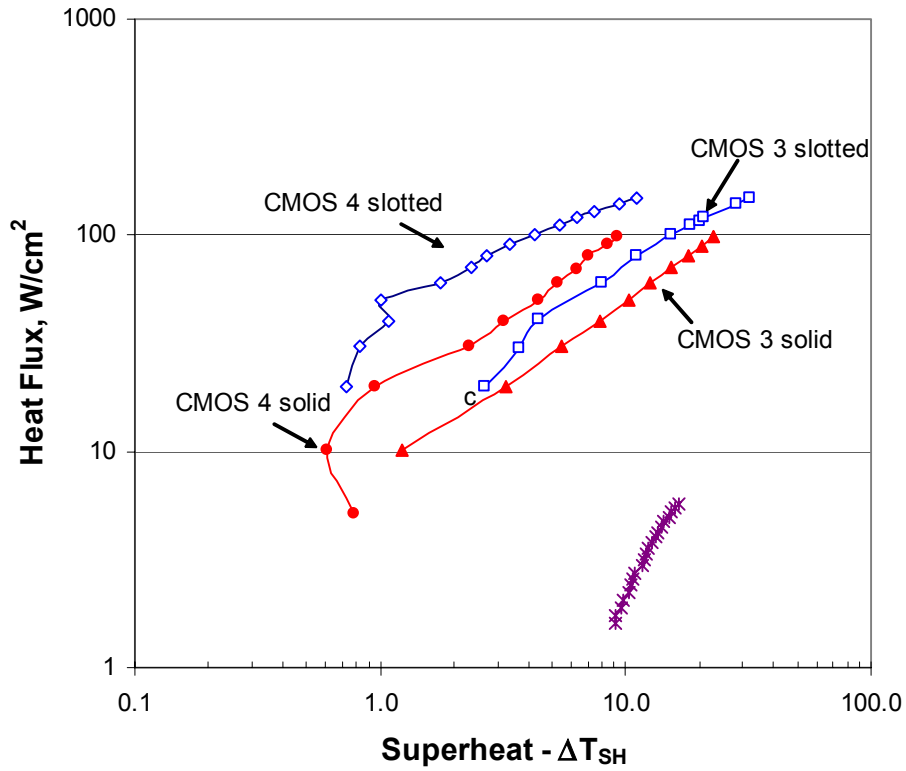


Figure 3. Plot of heat flux versus superheat for slotted and solid graphite foam evaporators.

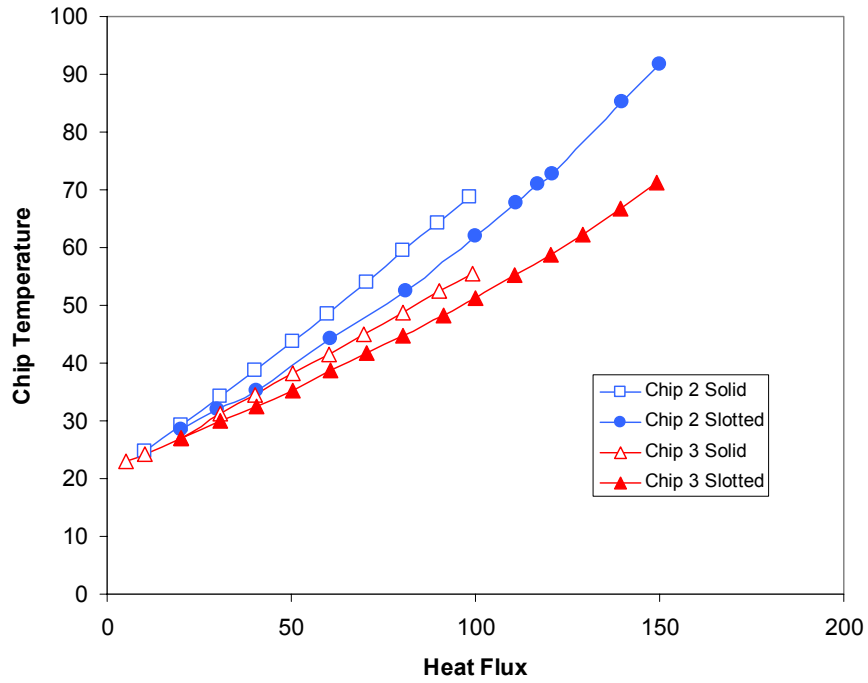


Figure 4. Plot of temperature of active layer on chip versus heat flux for slotted and solid graphite foam evaporators.

Table 1. Heat transfer performance of state-of-the-art thermosyphons and spray cooling techniques found in literature compared to that of the graphite foam thermosyphons.

Reference	Evaporator	Fluid	Heat Flux, q''	ΔT_{SH}	$R_{boil} \Delta T / q''$
3M [2]	None	FC-87	5.7 [†]	16.4	2.88
El-Genk [3]	Copper Surface	HFE-7100	22 [†]	28	1.27
Wei et al.[4]	Sintered Bronze Powder	R11	40 [†]	40	1.00
Ramaswamy [5]	Microchannel copper	FC-72	100 [†]	65	0.65
Rainey & You [6]	Microporous Diamond (DOM)	FC-72	27 [†]	13	0.48
Lin and Ponnappan [7]	SPRAY COOLING	FC-72	78 [†]	38	0.48
Nakayama [8]	Microchannel copper	FC-72	159 [†]	65	0.41
Coursey [1]	Poco HTC High Density Foam	FC-87	142.6 [‡]	51.2	0.36
Rainey and Lee [9]	Pin Finned Copper Block w/ Microporous Aluminum Coating	FC-72	140 [†]	38	0.27
This research	PocoFoam®	FC-72	118 [‡]	24	0.20
Lin and Ponnappan [7]	SPRAY COOLING	Water	480 [†]	48	0.1
This research	Slotted PocoFoam®	FC-87	149 [‡]	11	0.07

[†] CHF reached

[‡] CHF not reached

References.

1. Coursey, J., *Performance and Parametric Investigation of a Graphite Foam Thermosyphon Evaporator*, in *Mechanical Engineering*. 2003, University of Maryland: College Park. p. 93.
2. Tousignant, L., *3M Database*. 2004.
3. EL-Genk, M.S. and H. Bostanci, *Saturation boiling of HFE-7100 from a copper surface, simulating a microelectronic chip*. *International Journal of Heat and Mass Transfer*, 2003. **46**(10): p. 1841-1854.
4. Wu, W., et al., *Pool boiling heat transfer and simplified one-dimensional model for prediction on coated porous surfaces with vapor channels*. *International Journal of Heat and Mass Transfer*, 2002. **45**(5): p. 1117-1125.
5. Ramaswamy, C., Y. Joshi, and W. Nakayama, *Combined Effects of Sub-Cooling and Operating Pressure on the Performance of a Two-Chamber Thermosyphon*. *IEEE Transactions on Components, Packaging, and Manufacturing Technology-Part A*, 2000: p. 61-69.
6. Rainey, K.N. and S.M. You, *Effects of heater size and orientation on pool boiling heat transfer from microporous coated surfaces*. *International Journal of Heat and Mass Transfer*, 2001. **44**(14): p. 2589-2599.
7. Lin, L. and R. Ponnappan, *Heat Transfer Characteristics of Spray Cooling in a Closed Loop*. *Int. J. Heat Mass Transfer*, 2003. **46**: p. 3737-3746.
8. Nakayama, W., T. Nakajima, and S. Hirasawa, *Heat Sink Studs Having Enhanced Boiling Surfaces for Cooling Microelectronic Components*. *ASME Paper*, 1984(No. 84-WA/HT).
9. Rainey, K.N., S.M. You, and S. Lee, *Effect of pressure, subcooling, and dissolved gas on pool boiling heat transfer from microporous, square pin-finned surfaces in FC-72*. *International Journal of Heat and Mass Transfer*, 2003. **46**(1): p. 23-35.